DOSE-HOMOGENEITY DRIVEN BEAM DELIVERY SYSTEM PERFORMANCE REQUIREMENTS FOR MedAustron

Marcus Palm*, Fabian Moser, Michael Benedikt, CERN, 1211 Geneva, Switzerland
Adrian Fabich, EBG MedAustron, Wr. Neustadt, Austria

Abstract

MedAustron [1], the Austrian hadron therapy center is currently under construction. Irradiation will be performed using active scanning with proton and carbon ion pencil beams. Major beam delivery system contributors to dose heterogeneities are evaluated: beam position, beam size and spot weight errors. Their individual and combined effect on the dose distribution is quantified, using semi-analytical models of lateral beam spread in the nozzle and target and depth-dose curves for protons and carbon ions. Deduced requirements on critical parts of the beam delivery system are presented. Preventive and active methods to suppress the impact of beam delivery inaccuracies are proposed.

INTRODUCTION

MedAustron will provide proton and carbon ion beams for tumor therapy by means of active scanning. In order to specify performance requirements on vital aspects of the beam delivery system (BDS), such as synchrotron extraction stability or scanning magnet accuracy, the relation between BDS imperfections and resulting dose errors must be clear. In this paper, the resulting target dose errors from different types of beam delivery errors are summarized and fundamental BDS performance specifications based on clinical dose homogeneity requirements are presented.

Main parameters of the MedAustron BDS are summarized in Table 1.

Table 1: Main BDS Parameters of MedAustron

	Min	Max
Proton energy range [MeV]	60	250
Carbon energy range [MeV/n]	120	400
Protons per spill	1×10^9	1×10^{10}
Carbons ions per spill	4×10^7	4×10^8
Spill duration [s]	1.0	10
Beam FWHM at isocenter [mm]	4	10
Time to irradiate 1 spot [μs]	≥ 300	
Time to move between neighboring spots [μs]	≤ 200	

* e-mail: marcus.palm@cern.ch

METHODS

Scanning Method

In depth the target is divided into layers of a few mm, each layer corresponding to the penetration depth of a specific extraction energy. Every iso-energy layer is divided into spots and two orthogonal dipoles (scanning magnets) guide the beam from spot to spot during irradiation. The beam is fixed upon each spot until a pre-determined amount of dose has been delivered and then guided to the next spot. The distance δ between two neighboring spots is typically 1/3 of the FWHM (W) of the beam size.

Beam Delivery Imperfections

An example of the horizontal and vertical beam profile is shown in Fig. 1. In the vertical plane, the beam is Gaussian, while in the horizontal plane, the beam profile is trapezoidal due to the horizontal 3rd integer resonance extraction mechanism.
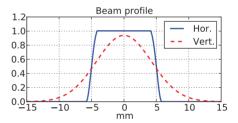

Figure 1: Horizontal and vertical beam profile at the isocenter (FWHM=10 mm, scattering is neglected).

In order to produce a homogeneous dose from overlapping Gaussian profiles, if suffices that $\delta \leq 0.7W$ [2]. The combined dose from overlapping trapezoids, however, can only be homogeneous if the unscattered FWHM is exactly an integer multiple of the spot-to-spot distance, i.e $\delta = W/n$. The horizontal width of the beam must therefore exactly match the spot-to-spot distance and an erroneous beam width would cause dose heterogeneities.

Other BDS sources of dose heterogeneity are random spot-to-spot errors of beam positioning (caused by current ripple in the scanning magnets), spot weights (caused by intensity fluctuations of the extracted beam) and beam size (caused by e.g. current ripple in optical elements along the transfer line).

08 Applications of Accelerators, Technology Transfer and Industrial Relations

U01 Medical Applications

Dose Homogeneity Calculations

In order to quantize the impact of mentioned beam delivery errors on dose homogeneity, a spot scanning dose calculator has been implemented. The 3-dimensional dose distribution of each spot i, $\phi_i(x, y, z)$, is calculated using the beam profiles (trapezoidal/Gaussian) given by the extraction process, a semi-empirical scattering model [3] and parameterized proton and carbon ion Bragg curves in water from GEANT4 simulations. An example of the dose distribution in the horizontal plane (y=0) of a single spot in water is shown in Fig. 2 for proton and carbon ions.

(a) 8 mm proton beam
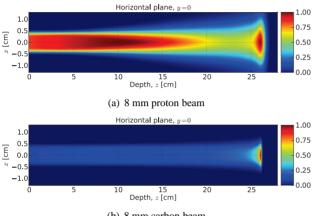

(b) 8 mm carbon beam

Figure 2: Normalized dose distribution, $\phi(x, y = 0, z)$, of a single spot in water ($W = 8$ mm) with 26 cm range. Top: protons. Bottom: carbon ions. Note that different color scales have been used.

The dose calculator generates a treatment plan for producing a homogeneous dose in a rectangular target in water. The impact of BDS errors is studied by applying intentional errors (position, weight, size) to the optimized treatment plan and then calculating the resulting dose errors in the target volume.

The standard deviation (rms) of the dose error, σ_D, should not exceed 3.5% [4] when *all* error sources are taken into account. In this paper, an upper limit of σ_D=2.0% is used, taking only mentioned BDS errors into account. Assuming these are independent from other error types, such as patient setup misalignments and range errors, a margin of 2.9% remains (quadratic addition).

RESULTS

Static Beam Width Errors

Fig. 3(a) shows the central dose distribution at the Bragg peak of a 3×3 cm^2 field (δ=3.33 mm, W=10 mm) with spots arranged in a conventional Cartesian grid. Each spot is subject to a small beam width error of ΔW=-0.25 mm in the horizontal and vertical plane. Vertical stripes of up to 2% local overdosage are seen where the edges of the trapezoidal beam profiles no longer overlap perfectly. Depending on the beam size, the relative dose error due to a

static beam width error can be as high as 8% per mm ΔW.

The high sensitivity to a static beam width error can be significantly suppressed by modifying the treatment planning spot grid, as seen in Fig. 3(b), where every second spot row has been shifted by a distance of $\delta/2$. The same spot width error has been applied, but since the sharp, mismatched, edges are no longer aligned vertically, the dose error is reduced to 0.3%.
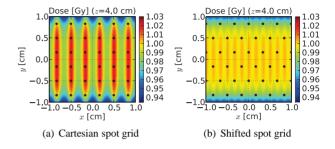

(a) Cartesian spot grid   (b) Shifted spot grid

Figure 3: Dose distribution with static beam width error $\Delta W = -0.25$ mm at all spots.

Integral Dose-driven Scanning

Two methods of deciding when to trigger the beam to move from spot i have been considered:

1. When spot i has received $N_i - N_{lag}$ particles, where N_i is the nominal spot dose and N_{lag} the expected number of particles delivered during the time it takes reach to the next spot.

2. When a *total* dose of $(\sum_{j=1}^{i} N_j) - N_{lag}$ has been delivered up to the i:th spot.

The final dose of spot i depends on how much the intensity fluctuates during the time it takes to reach the next spot. With Method 1, the dose counter must be reset each time the beam reaches a new spot, and the dose error at spot $i-1$ will be independent from the the dose error at spot i. With Method 2, however, an underdosage at spot $i-1$ forces the beam to stay longer at spot i, in order to reach the proper integral dose. Thus, the error delivered to one spot is automatically subtracted from the nominal dose of the next spot. One advantage with Method 2 is that low-frequency variations of the extracted particle rate are automatically compensated for: if the the beam intensity is only 80% of anticipated, $0.8\times N_{lag}$ particles will be delivered during spot transition. With Method 1, this would mean systematic under-dosage; with Method 2 only the first spot will be affected.

Random Spot Errors

The standard deviation of the dose error caused by beam delivery imperfections depends on many factors: beam type (proton/carbon ions), target shape, number of layers etc. The beam delivery system must be designed to deliver a homogeneous dose in all cases. The "worst case" target would be a single-layer target to be irradiated with a carbon ion beam, since carbon ion beam profiles are sharper

than protons and dose heterogeneities in the proximal part of multi-layer targets are statistically averaged out. In the random dose error calculations, a single layer at 4 cm depth has been assumed (taking scattering in the nozzle into account [3]). The standard deviation of the relative dose error, σ_D, has been calculated by applying uniformly distributed errors to the spot weights (relative weight errors within $\pm E_n$), spot positions ($\pm E_{pos}$) and beam widths ($\pm E_W$) for $\delta = W/3$ and a shifted spot grid. It is found that σ_D is linear to all three, and quadratic addition applies when combining different error types:

$$\sigma_D = \sqrt{(k_{pos}E_{pos})^2 + (k_W E_W)^2 + (k_n E_n)^2} \qquad (1)$$

where $k_{pos} = 0.08$ mm^{-1}, $k_W = 0.04$ mm^{-1} and $k_n = 0.10$ (for Method 2)[1] With equal contribution from all error sources and $\sigma_D \leq 2.0\%$, the BDS must ensure that:

$$\begin{cases} E_n \leq & 12\% \\ E_{pos} \leq & 0.15 \text{ mm} \\ E_W \leq & 0.3 \text{ mm} \end{cases} \qquad (2)$$

These conditions are sufficient for all beam sizes between 4 and 10 mm.

With a nominal carbon dose of 0.7 Gy (physical dose), about 400,000 ions per spot are needed, which takes 1 ms to deliver at maximum extraction intensity. For spot weight errors caused by intensity fluctuations during the 200 μs spot transition, intensity fluctuations of up to 60% would then be acceptable. This can, via the extraction mechanism, be translated into stability requirements on the synchrotron magnet currents of a few ppm.

The size of the scanning field is ± 100 mm, so the required positioning accuracy of ± 0.15 mm is equivalent to a scanning magnet current accuracy of ± 1500 ppm of maximum current. However, low energy protons require only 1/6 of the maximum scanning magnet current to reach the edges of the scanning field, which tightens the requirement to ± 250 ppm.

Benchmarking at PSI

The spot scanning dose calculator has been benchmarked in Gantry 2, PSI, Switzerland. The excellent agreement between simulated and measured dose error (using a CCD camera) is demonstrated in Fig. 4, which shows a transversal cross section of a proton field ($\delta = 3.0$ mm) subject to random spot weight errors of up to $\pm 40\%$. The widening of the proton beam with depth (measured by inserting Plexiglas plates in front of the camera) is accurately reproduced by the spot calculator.

CONCLUSIONS

A simple modification of the treatment planning spot grid significantly reduces the risk of static beam width er-

---

[1]k_n is lower for Method 2 than for Method 1 for spot grids where $\delta \lesssim W/2$: subtracting the weight error at one spot from the next is only beneficial if the spots are close together.

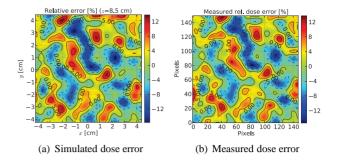(a) Simulated dose error   (b) Measured dose error

Figure 4: Error dose distribution: each spot is subject to a random weight error within $\pm 40\%$

rors causing over- or underdosage.

Implementing integral dose-driven scanning will make the beam delivery system robust against low-frequency variations of the beam intensity. It is also the preferred method for reducing dose heterogeneities caused by random beam intensity fluctuations.

To keep the standard deviation of the relative dose error below 2% in a "worst case" target (single layer, carbon ions) requires that intensity fluctuations (in a 200 μs integration window) are kept below 60%, that the current of the scanning magnet power supplies is accurate to within ± 250 ppm and that the beam width is constant within ± 0.3 mm from spot to spot. For more realistic, multiple layer-targets, these requirements can be relaxed.

An even higher tolerance to random spot errors than specified in Eq. 2 can be achieved with a tighter spot grid ($\delta = W/4$). This reduces the nominal spot doses by a factor 9/16 and may require using a lower extraction intensity, since no spot can be shorter than 300 μs. Whether the improved homogeneity of a tighter spot grid justifies the resulting increase in effective irradiation time must be judged from patient to patient.

ACKNOWLEDGMENTS

REFERENCES

[1] M. Benedikt and A. Wrulich, "MedAustron Project overview and status," *The European Physical Journal Plus*, vol. 126, pp. 1–11, 2011. 10.1140/epjp/i2011-11069-9.

[2] U. Weber and G. Kraft *Physics in Medicine and Biology*, vol. 44, no. 11, pp. 2765–2775, 1999.

[3] M. Palm, M. Benedikt, and A. Fabich, "Design Choices of the MedAustron Nozzles and Proton Gantry based on Modeling of Particle Scattering," in *Proceedings of IPAC'11, San Sebastian, Spain*, 2011.

[4] A. Wambersie, "What accuracy is required and can be achieved in radiation therapy," in *College on medical physics and workshop on nuclear data for science and technology: Medical applications*, 1999.